PNAS RESEARCH ARTICLE | APPLIED BIOLOGICAL SCIENCES

Comprehensive stable-isotope tracing of glucose and amino acids identifies metabolic by-products and their sources in CHO cell culture

Jacqueline E. Gonzalez[a,1], Harnish Mukesh Naik[b,1], Eleanor H. Oates[a], Venkata Gayatri Dhara[b], Brian O. McConnell[a], Swetha Kumar[b], Michael J. Betenbaugh[b], and Maciek R. Antoniewicz[a,c,2]

Affiliations are included on p. 9.

Edited by James Liao, Academia Sinica (Taiwan), Taipei, Taiwan; received February 14, 2024; accepted August 6, 2024

Mammalian cell culture processes are widely utilized for biotherapeutics production, disease diagnostics, and biosensors, and hence, should be optimized to support robust cell growth and viability. However, toxic by-products accumulate in cultures due to inefficiencies in metabolic activities and nutrient utilization. In this study, we applied comprehensive ^{13}C stable-isotope tracing of amino acids and glucose to two Immunoglobulin G (IgG) producing Chinese Hamster Ovary (CHO) cell lines to identify secreted by-products and trace their origins. CHO cells were cultured in media formulations missing a single amino acid or glucose supplemented with a ^{13}C-tracer of the missing substrate, followed by gas chromatography-mass spectrometry (GC-MS) analysis to track labeled carbon flows and identify by-products. We tracked the sources of all secreted by-products and verified the identity of 45 by-products, majority of which were derived from glucose, leucine, isoleucine, valine, tyrosine, tryptophan, methionine, and phenylalanine. In addition to by-products identified previously, we identified several metabolites including 2-hydroxyisovaleric acid, 2-aminobutyric acid, L-alloisoleucine, ketoisoleucine, 2-hydroxy-3-methylvaleric acid, desmeninol, and 2-aminobutyric acid. When added to CHO cell cultures at different concentrations, certain metabolites inhibited cell growth while others including 2-hydroxy acids, surprisingly, reduced lactate accumulation. In vitro enzymatic analysis indicated that 2-hydroxy acids were metabolized by lactate dehydrogenase suggesting a possible mechanism for lowered lactate accumulation, e.g., competitive substrate inhibition. The ^{13}C-labeling assisted metabolomics pipeline developed and the metabolites identified will serve as a springboard to reduce undesirable by-products accumulation and alleviate inefficient substrate utilization in mammalian cultures used for biomanufacturing and other applications through altered media formulations and pathway engineering strategies.

amino acid catabolism | mammalian cell culture | stable isotope labeling | metabolic by-products | mass spectrometry

Significance

Mammalian cells are widely used for biomedicines production and as therapies. To grow, cells require critical nutrients including glucose and amino acids. However, these nutrients may also be converted into undesirable by-products that can be toxic to cells. Therefore, in order to track the source and formation of these by-products, individual amino acids and glucose were labeled with stable isotopes containing heavy nontoxic carbon atoms. Advanced mass spectrometry tools were applied to identify metabolic by-products and their sources. Specific by-products inhibited cell growth while others reduced lactate accumulation. Techniques developed and by-products identified will be used to lower formation of undesirable metabolites to create healthier, more productive cell cultures so manufacturing of biomedicines can be optimized to meet global demand.

Mammalian cells are used for a myriad of applications including production of biotherapeutics ranging from monoclonal antibodies to cell and gene therapies to viral vaccines (1, 2). They are also used as biosensors to probe the presence of various disease markers in the human body, thereby, aiding in disease diagnosis (3). Furthermore, mammalian cell-based assays are used to detect the presence of pathogens in clinical, environmental, and food samples (4). Mammalian cell cultures also serve as model test systems for studying physiology and biochemical pathways to investigate disease causation (5). A key part of successful mammalian cell culture is to provide the media and environment that ensure robust growth for the specific purpose or application. Indeed, efforts to optimize media formulations and advance processing technologies such as periodic feeding, cell retention, and enhanced at-line monitoring and control have yielded substantial improvements in mammalian cell performance in cultures that can result in very high cell densities and extended cultivation times for biomanufacturing and other applications (6–10).

However, these intensified mammalian cell culture processes can result in the accumulation of potentially toxic metabolic by-products, especially for fed-batch mammalian cell culture processes with extended cultivation periods widely used in biomanufacturing (11, 12). Indeed, well-known metabolic by-products such as lactate and ammonia have been shown over many years to negatively impact cell growth, productivity, and, in the case of ammonia, product quality including glycosylation (13, 14). Once identified, approaches can be implemented to limit their impact including the use of glutamine-synthase (GS) cell lines to reduce ammonia accumulation, genetic engineering to alter expression of

Competing interest statement: Current employment of authors: J.E.G. is currently affiliated with Takeda Pharmaceutical Company; H.M.N. is currently affiliated with IQVIA; E.H.O. is currently affiliated with Genentech; V.G.D. is currently affiliated with Pfizer; B.O.M. is currently affiliated with Amgen; S.K. is currently affiliated with Sanofi.

This article is a PNAS Direct Submission.

[1]J.E.G. and H.M.N. contributed equally to this work.

[2]To whom correspondence may be addressed. Email: mranton@umich.edu.

This article contains supporting information online at https://www.pnas.org/lookup/suppl/doi:10.1073/pnas.2403033121/-/DCSupplemental.

Published October 4, 2024.

enzymes such as pyruvate kinase muscle (PKM), pyruvate dehydrogenase kinases (PDHks), and malate dehydrogenase-2 (MDH-2) (15–17) as well as process modifications including high-end pH-controlled delivery of glucose (HIPDOG) to reduce lactate accumulation (18). However, while ammonia and lactate are the most well-known by-products, the potential exists for other metabolic by-products to accumulate in mammalian cell cultures, especially at the high cell densities prevalent in intensified mammalian cell culture bioproduction.

Mammalian cells cultivated at high cell densities will consume large amounts of nutrients including both glucose and amino acids. Therefore, methods are needed to help identify these additional metabolic by-products and in order to ascertain their chemical nature, their levels in culture, their sources if possible, and ultimately their impact on mammalian cell culture performance. A few follow-up studies have sought to identify toxic metabolic by-products beyond lactate and ammonia (11, 12). Mulukutla et al. identified nine metabolic by-products including indole 3-carboxylate, 4-hydroxyphenylpyruvate, homocysteine, 2-hydroxybutyrate, 3-(4-hydroxyphenyl) lactate, phenyllactate, indole-3-lactate, formate, and isovalerate using an LC-MS and GC-MS-based global metabolite profiling approach. Interestingly, a number of these metabolites, including catabolic intermediates or metabolic by-products of phenylalanine, tyrosine, tryptophan, leucine, serine, threonine, methionine, or glycine metabolism, inhibited GS-Chinese Hamster Ovary (GS-CHO) cell growth at certain concentrations (11). In another study, our group identified growth-inhibiting metabolic by-products generated through the polyamine pathway, nucleotide metabolism, and nicotinamide metabolism in addition to amino acids pathway degradation products using an LC-MS/MS-based untargeted metabolomics platform (12). This study determined that aconitic acid, 2-hydroxyisocaproic acid, methylsuccinic acid, cytidine monophosphate, trigonelline, n-acetyl putrescine, indole-3-carboxylic acid, and guanosine monophosphate had a negative impact on at least one of the following—growth, productivity, or glycosylation (12). Thus, accumulation of metabolic by-products beyond ammonia and lactate can significantly hinder cell culture performance. Hence, it would be valuable to further develop and augment techniques to identify mammalian cell culture metabolic by-products beyond the current known compounds and to characterize their impact on cell culture performance.

Unfolding the correlation between such downstream metabolic by-products and their upstream feeding source can then potentially be applied to minimize their negative impacts and improve mammalian cell culture–based biomanufacturing by improving basal medium and feed formulations, genetic engineering of cell lines, and improving process control to limit overfeeding of amino acids in cell culture. Indeed, Mulukutla et al. controlled the accumulation of toxic metabolic by-products by limiting excessive amino acid concentration in basal media and feed as well as by knocking out genes responsible for production of specific metabolic by-products using microRNA (miRNA) based RNA interference (RNAi) technology (19). In another study, our group modified basal medium and feed composition through a design of experiments approach and response surface design analysis to limit accumulation of toxic metabolic by-products and improve peak viable cell densities and IgG production (20). Thus, identifying metabolic by-products may help in the design of approaches to reduce or eliminate their accumulation from cell cultures, ultimately leading to methods to enhance cell viabilities and cell culture performance in high-density cultures used in recombinant protein production, viral processing, and cell therapies. In addition, such approaches may lower raw material costs and operational costs by reducing the inputs for these increasingly important bioproduction events.

While previous studies have employed LC-MS- and GC-MS-based untargeted and targeted metabolomics to identify metabolic by-products, such MS-based metabolomics only enable measurements of relative abundance of metabolic by-products and do not provide information on nutrient sources or substrates and metabolic activities leading to the production of metabolic by-products. Stable-isotope labeling of nutrients or substrates can be used for identification of reaction networks and a more comprehensive assessment of intracellular metabolic activity leading to generation of by-products in mammalian cells. When a ^{13}C-labeled substrate such as glucose or a specific amino acid is added to cell culture and subsequently metabolized, ^{13}C-labeling from the substrate is incorporated into metabolic products and by-products endogenously synthesized from the ^{13}C-labeled substrate (21, 22). Such metabolic products and by-products will become increasingly enriched with ^{13}C-labeling over time until the point where the ^{13}C-enrichment is stable over time. ^{13}C-labeling can then be tracked using mass spectrometry and, as a result, the carbon sources used by cells as well as the potential metabolic pathways can be identified based on observed mass isotopomers (23). Historically, for since almost two decades now, ^{13}C-labeled substrates have been used in the form of ^{13}C-labeled biomass as an internal reference or standard to quantify intracellular and extracellular metabolite concentrations in biological systems (24). More recently, in microbial and mammalian cell cultures, stable-isotope labeling, typically ^{13}C-labeling, has been used primarily for metabolic flux analysis (^{13}C-MFA) to understand cellular performance under different media conditions and varying process parameters (25, 26) and to uncover signaling pathways especially in cancer cells (27–29) and novel metabolic pathways in microorganisms (30–32). Such studies typically employ isotopic labeling in a targeted fashion to elucidate certain pathways of interest, determine only a subset of metabolic activities, and identify by-products of a few specific isotopic tracers such as ^{13}C-glucose and ^{13}C-glutamine. To our knowledge, only one previous study has applied comprehensive ^{13}C-labeling in mammalian cells to detect endogenous metabolites, assess activities of metabolic pathways, and determine sources of biomass and metabolic by-products in cancer cells (33).

A comprehensive and global ^{13}C stable-isotope tracing metabolomics pipeline with the potential to unravel intricacies of metabolism has not been previously applied to mammalian cell cultures used in biomanufacturing and biomedical applications. Our study employs an inclusive amino acid and glucose ^{13}C-labeling approach to identify secreted metabolic by-products and their sources in mammalian cell cultures used for producing biologics. Specifically, in this study, we applied ^{13}C-labeling assisted metabolomics to identify metabolic by-products and the source of these by-products by feeding ^{13}C-labeled glucose and ^{13}C-labeled amino acids in batch cell cultures of two different mammalian cell lines—CHO-K1 and GS-CHO. We supplemented custom media formulations each missing a single amino acid or glucose with a universally labeled ^{13}C-tracer of the missing amino acid or glucose. Cells were grown in batch mode and GC-MS analytical methods were used to track the labeled carbon flows throughout the growth phase to identify by-products secreted by CHO cells. Commercially available standards were then used to verify the identity of 45 secreted metabolites. Pathway mapping coupled with ^{13}C-labeling of substrates enabled us to determine the substrate sources, metabolic pathways, and enzymes responsible for the generation of many of these by-products. Interestingly, when added to CHO cell batch cultures, we observed that certain metabolites inhibited cell growth while other metabolites, surprisingly, limited lactate accumulation, suggesting that not all metabolic by-products are growth-inhibiting in nature. Taken together, the analytical methods developed and

implemented here and the metabolites identified will serve as a worthwhile starting point and approach to identify metabolic by-products from a range of mammalian cell culture systems. Furthermore, such knowledge can be used to address and alleviate inefficient substrate utilization and metabolic toxicities arising in numerous current and emerging mammalian bioproduction platforms through complementary pathway engineering strategies, media, and feed optimization, and online monitoring of amino acids levels in culture in order to alter cell physiology to divert these substrates away from synthesis of toxic metabolic by-products for improved performance in biologics manufacturing and other applications.

Results

Global Stable-Isotope Tracing Identifies Metabolic By-Products Derived from Glucose and Amino Acids. To better understand what small molecules are secreted by mammalian cells in culture, as well as their sources, we conducted all-encompassing carbon isotope-tracing studies using two mammalian cell lines, CHO-K1 and GS-CHO, each producing recombinant IgGs. CHO cells were grown in 21 and 20 separate batch cultures, respectively, using chemically defined media in which one specific substrate was fully ^{13}C-labeled, either glucose or a specific amino acid (Fig. 1*A*). No glutamine tracer was used with GS-CHO cells since these cells have a heterologous glutamine synthetase (GS) gene. Spent media samples were collected on days 0 and 5, chemically treated [MOX (2% methoxyamine·HCl in pyridine)-TBDMS (*tert*-butyldimethylsilyl chloride) derivatization] (34), and subjected to GC-MS analysis. In total, 214 peaks were identified in the total ion chromatograms of spent media with 91 peaks exhibiting increasing intensity, 91 peaks exhibiting decreasing intensity, and 32 peaks with unchanged intensity (less than 20% change between days 0 and 5) (Fig. 1*A*).

The 91 peaks with decreased intensity presumably corresponded to metabolites that were consumed by CHO cells. To verify this, we analyzed each medium before and after supplementation with ^{13}C-tracers (Fig. 1*B*). Of the 91 peaks, 38 were glucose derivatives, 49 were amino acid derivatives, 3 were labeled compounds that were formed from amino acids during the chemical derivatization procedure, and one was an unlabeled medium component that was later determined to be pyruvate. To identify the metabolic origins of the other peaks, we analyzed mass spectra of each peak from each of the tracer experiments. Because a different substrate was ^{13}C-labeled in each tracer experiment (i.e., either glucose or an amino acid), if a particular metabolite was derived from a specific ^{13}C-labeled substrate, then we would expect to observe a shift in *m/z* values due to the incorporation of ^{13}C-atoms from that tracer. An example is shown in Fig. 1*C*, where the main ion in the mass spectrum was *m/z* 202 for all experiments except for tracer experiment with [U-^{13}C]valine, where the main ion was shifted to *m/z* 207, thus indicating that this compound was derived from valine and contained five ^{13}C-labeled atoms (i.e., M+5). This procedure enabled us to determine the sources of all peaks (Fig. 1*D*). Of the 91 peaks with increasing intensity, 84 peaks incorporated ^{13}C-labeling from at least one of the tracers. Of the 32 peaks that remained unchanged, none became ^{13}C-labeled (Fig. 1*C*), suggesting that they were not metabolic by-products. By analyzing the total ion chromatogram of pure water as a control (after MOX-TBDMS derivatization), we confirmed that 19 of the 32 peaks were chemical impurities or artifacts of the MOX-TBDMS derivatization procedure, and the remaining 13 were other unknown compounds present in our cell culture media.

Metabolic By-Products Derived from Glucose Are Produced in Core Metabolic Pathways. To determine the identity of compounds corresponding to each peak, we took advantage of the fact that (MOX-)TBDMS derivatives produce characteristic fragments in GC-MS analysis (Fig. 2*A*). Specifically, one of the most abundant ions in the mass spectra of (MOX-)TBDMS derivatives is the M-57 ion (resulting from the loss of C_4H_9 from the TBDMS side group), where M is the molecular weight of the derivatized molecule. The MOX treatment in the first derivatization step protects ketone groups (Fig. 2*A*); without this step, compounds containing ketone groups are difficult to detect by mass spectrometry. As outlined in Fig. 2*B*, we were able to assign putative metabolites for many peaks based on their molecular size and mass isotopomer distribution. We then verified the identity of 45 of these metabolic by-products using pure analytical standards (Dataset S1).

A large number of metabolic by-products that incorporated ^{13}C-labeling from glucose were derived from core metabolic

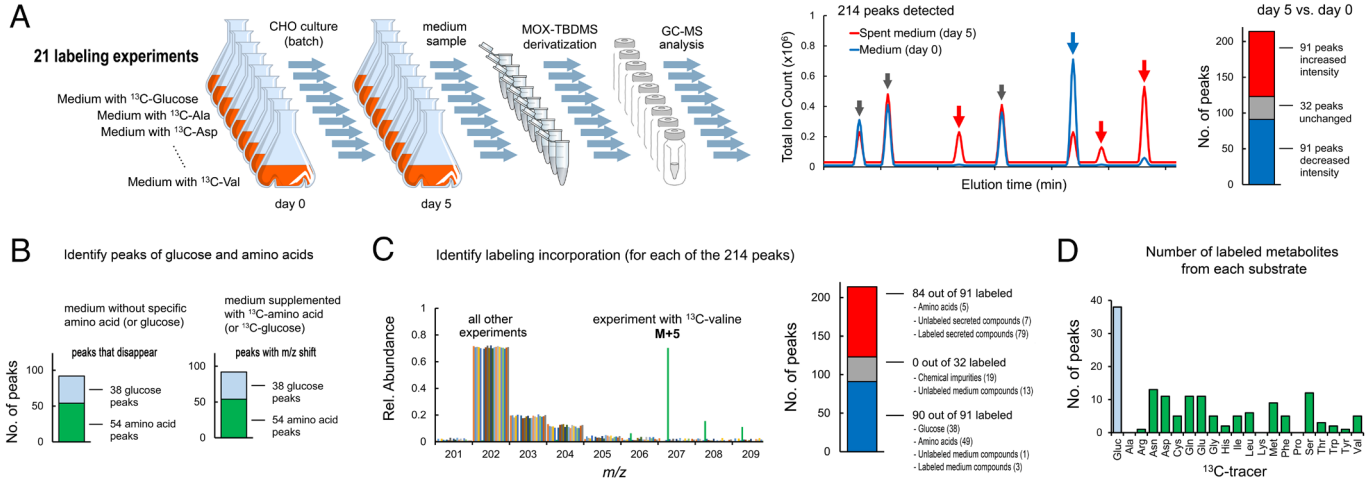

Fig. 1. Comprehensive stable-isotope tracing identifies metabolic by-products derived from glucose and amino acids. (*A*) CHO cells were grown in 21 parallel cultures using custom media, each containing a different ^{13}C-tracer, either glucose or an amino acid. Supernatant samples were collected on days 0 and 5 and analyzed by GC-MS to identify peaks in the chromatogram that either increased, decreased, or remained unchanged (less than 20% change) in intensity. (*B*) GC-MS analysis of media before and after addition of ^{13}C-tracers identified all peaks in the chromatogram that corresponded to glucose and amino acids. (*C*) Analysis of shifts in *m/z* (i.e., increases in mass from the incorporation of ^{13}C atoms) from 21 tracer experiments identified the sources for each peak in the chromatogram. (*D*) Number of peaks in the chromatogram with a shift in *m/z* for each of the 21 tracer experiments.

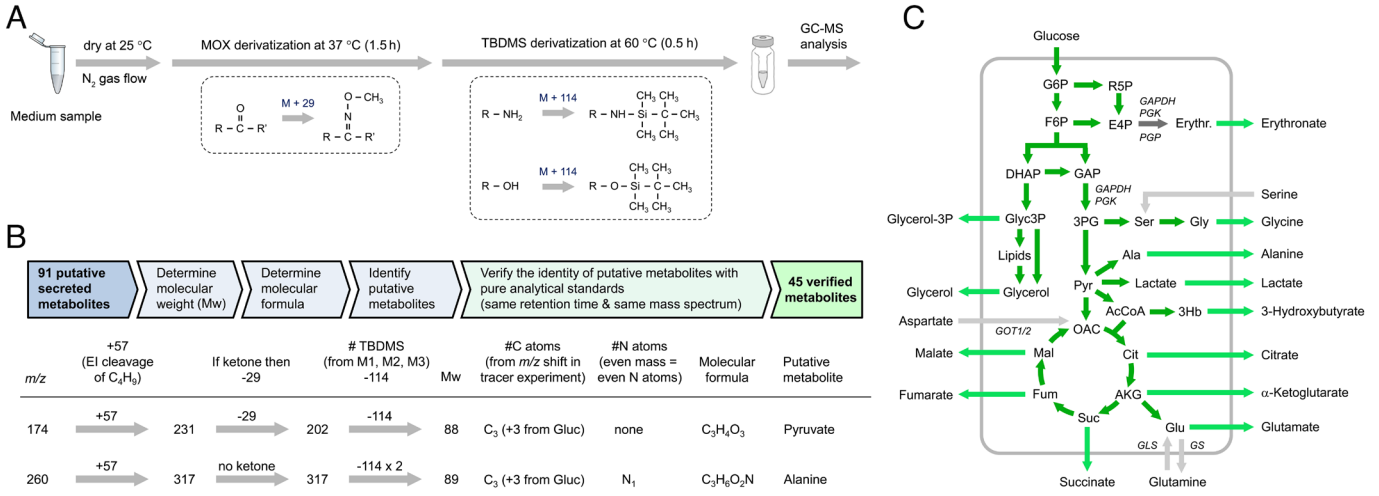

Fig. 2. Identification and verification of secreted metabolites. (*A*) Medium samples were dried, treated with MOX (to protect ketone groups) and TBDMS (to derivatize hydrophilic groups), and then analyzed by GC-MS. (*B*) To determine the identity of the peaks in the chromatogram, mass spectra were analyzed to determine the chemical formula and postulate potential compounds. To confirm the identity of the metabolites, pure analytical standards were purchased and analyzed by GC-MS. (*C*) Most of the extracellular metabolites that originated from glucose were produced in core metabolic pathways. Abbreviations: GAPDH: glyceraldehyde-3-phosphate dehydrogenase; PGK: phosphoglycerate kinase; GOT1/2: glutamic-oxaloacetic transaminase 1, 2; GLS: glutaminase; GS: glutamine synthase.

pathways, such as glycolysis and the TCA cycle (Fig. 2*C*). These metabolic by-products included lactate, glutamate, alanine, glycine, glycerol, glycerol-3-phosphate, citrate, a-ketoglutarate, succinate, fumarate, and malate. Many of these metabolites have been reported previously (35–38). We also identified two additional metabolites derived from glucose not previously reported for CHO cell cultures, 3-hydroxybutyrate and erythronate. 3-hydroxybutyrate is a ketone body that is primarily synthesized in liver cells from acetyl-CoA, although it can also be produced from partial-degradation of branched-chain amino acids (BCAAs) (39, 40). In our tracer experiments, 3-hydroxybutyrate only became labeled from ^{13}C-glucose, indicating that it was synthesized de novo from acetyl-CoA and not derived from degradation of BCAAs. Erythronate is not a typical product of mammalian metabolism. A recent study determined that erythronate can be produced by mammalian cells from the pentose phosphate pathway intermediate erythrose 4-phosphate (E4P) (41), as the result of promiscuous activity of two glycolytic enzymes, glyceraldehyde phosphate dehydrogenase (GAPDH) and phosphoglycerate kinase (PGK). In glycolysis, GAPDH and PGK catalyze the conversion of glyceraldehyde 3-phosphate (GAP) to 3-phosphoglycerate (3PG) (Fig. 2*C*). Collard et al. (41) demonstrated that these two enzymes can also convert E4P to 4-phosphoerythronate, which is then dephosphorylated by the enzyme phosphoglycolate phosphatase (PGP) to produce erythronate. Interestingly, it was shown that 4-phosphoerythronate strongly inhibits the oxidative pentose phosphate pathway enzyme 6-phospho-gluconate dehydrogenase (6PGDH). As such, PGP can play an important role in regulating glucose metabolism in mammalian cells.

Metabolic By-Products Derived from Amino Acids Result from Promiscuous Activity of Enzymes. Overall, the majority of metabolic by-products identified in this study were derived from the metabolism of amino acids, i.e., 50 out of 91 peaks with increasing intensity. This included previously reported by-products, such as 2-methylbutyric acid, isovaleric acid, homocysteine, 2-hydroxybutyric acid, phenyllactic acid, indolelactic acid, p-hydroxyphenyllactic acid, ketovaline, ketoleucine, o-tyrosine, 2-hydroxyisocaproic acid, and phenylacetic acid (11, 12, 42). In addition, we identified a number of additional metabolites derived from amino acids not previously reported for CHO cells, including 2-hydroxyisovaleric acid (derived from valine); L-alloisoleucine, ketoisoleucine, and 2-hydroxy-3-methylvaleric acid (derived from isoleucine); desmeninol and 2-aminobutyric acid (derived from methionine); and citrulline/ornithine (derived from arginine) (Fig. 3*A*).

Most of these metabolites are not found in the canonical pathways for amino acid breakdown in mammalian cells (green arrows in Fig. 3*B*). To explain the presence of these metabolites, we hypothesized alternative noncanonical metabolic reactions (red arrows in Fig. 3*B*). For example, we identified a large number of secreted 2-hydroxy acids, all of which had corresponding 2-keto acids that were part of canonical amino acid degradation pathways (Fig. 3*B*). This led us to hypothesize that these 2-hydroxy acids were likely produced by promiscuous activity of one or more dehydrogenases, such as lactate dehydrogenase (LDH) (43), or C-terminal binding proteins (CtBPs), which have been shown to display dehydrogenase activity and have been implicated in the production of desmeninol and possibly other 2-hydroxy acids (44, 45).

The metabolites isovaleric acid, 2-methylbutyric acid, and isobutyric acid (derived from leucine, isoleucine, and valine, respectively) were likely produced from isovaleryl-CoA, 2-methylbutyryl-CoA, and isobutyryl-CoA, all of which are intermediates in the canonical breakdown pathways of BCAAs (Fig. 3*B*). The promiscuous enzyme likely responsible for the formation of these metabolites is acyl-CoA thioesterase (ACOT) (46, 47), which natively metabolizes acyl-CoA esters to the corresponding nonesterified acid and coenzyme A.

A possible mechanism for the production of another metabolic by-product, L-alloisoleucine from isoleucine was proposed three decades ago by Mamer and Reimer (43), who suggested that L-alloisoleucine is an inherently unavoidable by-product of isoleucine transamination catalyzed by the enzyme branched-chain amino acid aminotransferase (BCAT), the first enzyme in the breakdown of isoleucine. This was supported by the observation that L-alloisoleucine levels are elevated in individuals with maple syrup urine disease (48), a genetic disorder characterized by deficiency in the branched-chain keto acid dehydrogenase (BCKDH) enzyme complex, the second step in the breakdown of isoleucine (Fig. 3*B*).

The mechanism for the formation of o-tyrosine from phenylalanine is still not completely understood. It could be enzymatic, or nonenzymatic. In the canonical pathway for the breakdown of phenylalanine, enzymatic oxidation of phenylalanine by

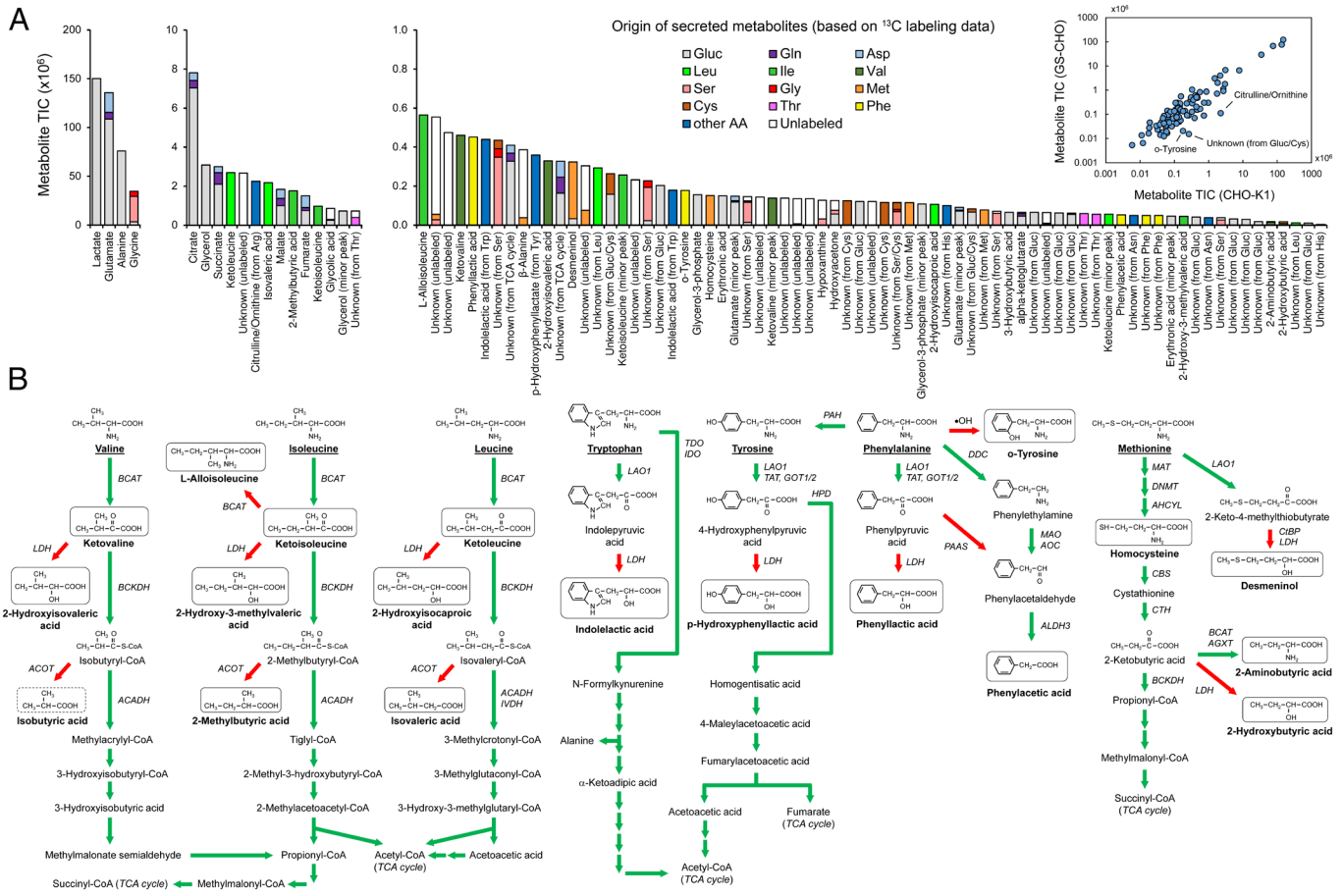

Fig. 3. Metabolic by-products derived from amino acids result from promiscuous activity of enzymes. (*A*) Secreted metabolic by-products from CHO-K1 cells and their sources, ordered from highest to lowest abundance based on TIC from GC-MS analysis of day 5 medium samples. Insert shows the comparison of TIC of secreted by-products from CHO-K1 cells and GC-CHO cells in batch culture. (*B*) Canonical metabolic degradation pathways of amino acids (green arrows) and hypothesized enzymatic reactions (red arrows) responsible for the production of identified metabolic by-products (boxed metabolites in bold text). Abbreviations: MAT: methionine adenosyltransferase; DNMT: DNA methyltransferase; AHCYL: adenosylhomocysteinase; CBS: cystathionine beta-synthase; CTH: cystathionine gamma-lyase; BCAT: branched-chain amino acid aminotransferase; AGXT: alanine-glyoxylate transaminase; TAT: tyrosine aminotransferase; BCKDH: branched-chain keto acid dehydrogenase; ACADH: acyl-CoA dehydrogenase; IVDH: isovaleryl-CoA dehydrogenase; ALDH3: aldehyde dehydrogenase 3; GOT1/2: glutamic-oxaloacetic transaminase 1, 2; LAO1: L-amino acid oxidase 1; PAH: phenylalanine hydroxylase; HPD: 4-hydroxyphenylpyruvate dioxygenase; TDO: tryptophan 2,3-dioxygenase; IDO: indoleamine 2,3-dioxygenase; CtBP: C-terminal binding protein; LDH: lactate dehydrogenase; DDC: dopa decarboxylase; MAO: monoamine oxidase; AOC: amine oxidase; ACOT: acyl-CoA thioesterase; PAAS: phenylacetaldehyde synthase.

phenylalanine hydroxylase (PAH) occurs on carbon 4 and produces p-tyrosine. However, some studies have suggested that PAH and tyrosine hydroxylase can also catalyze the formation of o-tyrosine and m-tyrosine from phenylalanine (49–51). Other studies have proposed that o-tyrosine and m-tyrosine could be produced non-enzymatically when hydroxyl radicals oxidize the benzyl ring of phenylalanine, resulting in formation of o-tyrosine and to a lesser extent m-tyrosine (49). Interestingly, we only found o-tyrosine in the spent media of our CHO cell cultures. If m-tyrosine was produced, it was below the detection limit of our instruments.

Several other metabolites that accumulated in our CHO cell cultures were ^{13}C-labeled from [U-^{13}C]threonine, [U-^{13}C]histidine, [U-^{13}C]serine, or [U-^{13}C]cysteine. However, due to limited availability of analytical standards, we could not verify the identity of these secreted by-products. These secreted by-products can be identified as part of future work in order to elucidate the metabolic fate of their amino acid sources.

When comparing the relative levels of metabolic by-products present in spent media for the two different CHO cell lines, we found that they were highly consistent (*Inset* in Fig. 3*A*). With only a few exceptions, the total ion counts (TIC) were within threefold for CHO-K1 cells and GS-CHO cells on day 5 of culture. The notable exceptions were the significantly higher levels of citrulline/ornithine (20-fold higher) and o-tyrosine (ninefold higher) in the spent media of CHO-K1 cells. These differences could be due to differences in growth rate, medium composition (i.e., glutamine was not present in the medium for GS-CHO cells), or sample collection timing. Overall, however, our results suggest that CHO cells secrete a similar set of metabolic by-products at comparable levels in batch cultures.

The two CHO cell lines were also grown in fed-batch to study the dynamics of metabolite by-product secretion under industrially relevant culture conditions from growth phase to stationary phase. CHO cells were cultured until cell viability dropped below 60%, which was 11 d for GS-CHO fed-batch culture and 22 d for CHO-K1 fed-batch culture. Metabolic by-product levels were quantified daily by GC-MS (Dataset S2). We observed that the majority of metabolic by-products continued to accumulate throughout the fed-batch cultures. Notable exceptions were 2-keto acids ketovaline, ketoleucine, and ketoisoleucine, which peaked during the growth phase and were then largely reconsumed during the stationary phase. Most of the 2-hydroxy acids, including indolelactic acid, desmeninol, phenyllactic acid, 2-hydroxyisocaproic acid, and p-hydroxyphenyllactic acid, accumulated at the highest rate during the growth phase, but then remained relatively constant, or even decreased slightly, during the stationary phase. Overall,

metabolic by-products that accumulated to the highest levels were derived from glucose metabolism in central metabolic pathways, which included glycerol (up to 3 mM), citrate (up to 1.5 mM), malate (up to 0.6 mM), and fumarate (up to 0.3 mM). The two most abundant metabolic by-products derived from amino acids were 2-methylbutyric acid and isovaleric acid, which accumulated to about 0.5 mM at the end of fed-batch cultures for both CHO cell lines. Previously, Mulukutla et al. reported that these two metabolites were also the most abundant metabolic by-products in four industrial CHO cell lines, with levels ranging from 1.6 to 2.4 mM for 2-methylbutyric acid and 1.0 to 2.7 mM for isovaleric acid (19). In our fed-batch cultures, all of the other metabolic by-products accumulated to levels less than 0.1 mM. Based on this, we estimated that less than 2% of amino acids were metabolized to metabolic by-products. However, it should be noted that these secreted by-products can be toxic even in small amounts. Hence, it is not so much about the fraction of each amino acid degraded to generate these secreted by-products but their ability to impact cell growth and metabolism even at low levels.

Sensitivity of CHO Cells to Secreted By-Products Is Cell Line Dependent. Previous studies have indicated that metabolic by-products derived from the partial breakdown of amino acids can have negative effects on CHO cell cultures (11, 12). To evaluate the potential toxicity of such compounds, we evaluated the impact of 20 of the identified metabolic by-products on CHO cell performance, including eight 2-hydroxy acids, three 2-keto acids, four nonproteinogenic amino acids, and five organic acids (Fig. 4*A*).

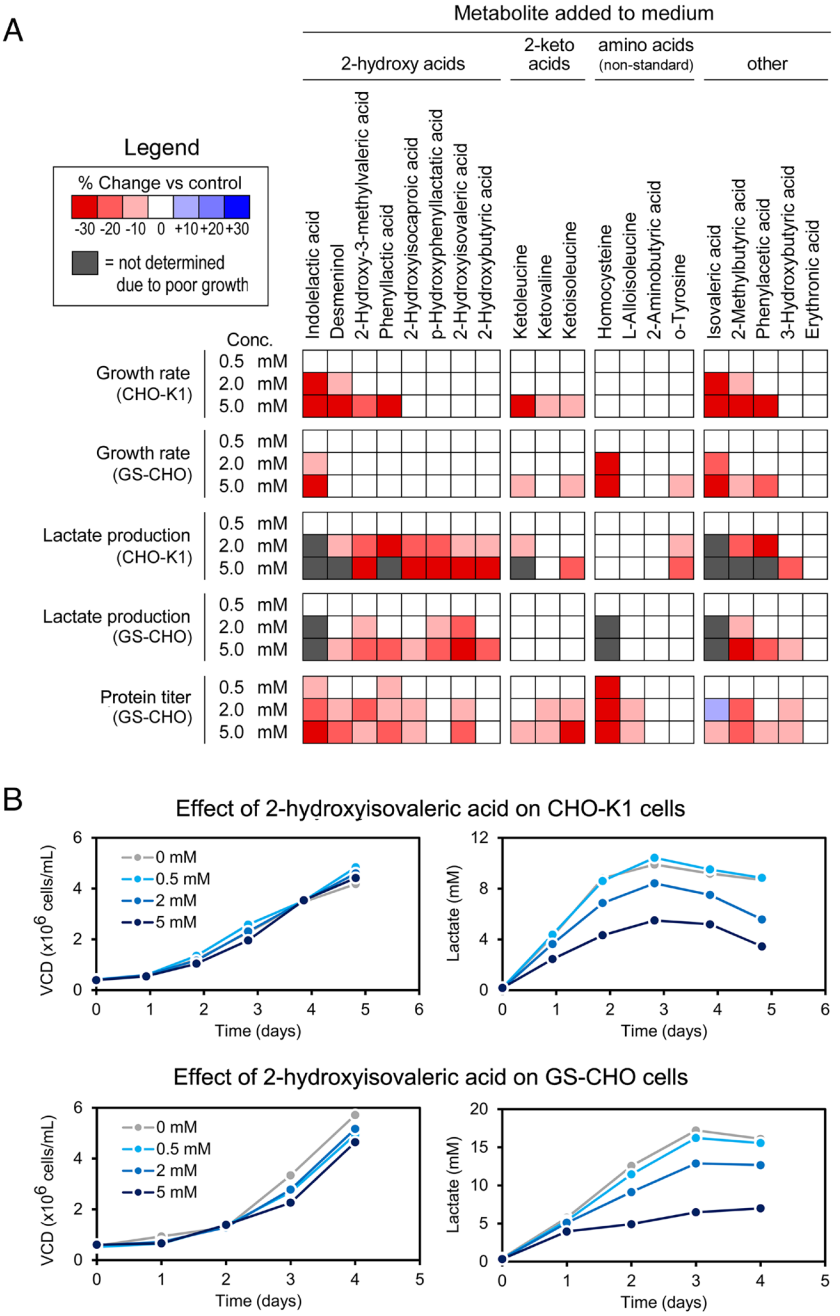

Fig. 4. Sensitivity of CHO cells to secreted by-products and their impact on lactate production. (*A*) Batch cultures were performed with two CHO cell lines, CHO-K1 and GS-CHO. In each culture, one of 20 metabolic by-products was added at either 0.5, 2, or 5 mM. Growth rates and lactate production were monitored and compared against control experiments without any metabolites added. (*B*) Many 2-hydroxy acids, including 2-hydroxyisovaleric acid (shown here), reduced lactate production without impacting cell growth.

Batch cultures were performed with the two CHO cell lines and each compound was added to media at three concentrations, 0.5, 2, and 5 mM, relevant in high-density cell cultures. At 0.5 mM, none of the metabolites altered growth rate compared to control cultures by more than 10% (Fig. 4*A*). However, at concentrations of 2 and 5 mM several metabolites inhibited cell growth. Two of the most toxic compounds were isovaleric acid and indolelactic acid, significantly inhibiting growth at 2 mM, while several organic acids were toxic at 5 mM for both cell lines. Interestingly, homocysteine was toxic at 2 mM to GS-CHO cells (Fig. 4*A*), but had no effect on the growth of CHO-K1 cells (even at 5 mM, Fig. 4*A*), indicating that CHO-K1 cells potentially recycle, reutilize, or redirect homocysteine to other pathways. In contrast, several 2-hydroxy acids were toxic to CHO-K1 cells at 5 mM, but had little or no effect on the growth of GS-CHO cells (Fig. 4*A*), suggesting potential rewiring by GS-CHO cells to utilize or tolerate 2-hydroxy acids.

Consistent with our findings, Mulukutla et al. (11, 19) demonstrated toxicity of homocysteine (at 0.5 mM), isovaleric acid (at 1 mM), phenyllactic acid (at 5 mM), and 2-methylbutyric acid (at 1 mM) in a commercial GS-CHO cell line. Interestingly, the same study reported no growth inhibition for indolelactic acid (up to 3 mM), although we observed significant growth inhibition at 2 mM with both our CHO cell lines. In addition, Mulukutla et al. observed toxicity of p-hydroxyphenyllactic acid (at 0.25 mM) and 2-hydroxybutyric acid (at 5 mM), while no growth inhibition was observed up to 5 mM with both our CHO cell lines.

We observed that product titers were reduced by about 10 to 20% by many metabolic by-products when added to cultures at high concentrations (2 and 5 mM) (Fig. 4*A*). However, when added at a low level (0.5 mM), product titers were not significantly affected, except by homocysteine, indolelactic acid, and phenyllactic acid (Fig. 4*A*).

2-Hydroxy Acids Reduce Lactate Production in CHO Cell Cultures and Are Likely Produced by LDH. Although none of the metabolites enhanced CHO growth rates, some metabolites were observed to significantly lower lactate accumulation (Fig. 4). In particular, multiple 2-hydroxy acids reduced the production of lactate by as much as 60%, e.g., 2-hydroxyisovaleric acid at 5 mM, without significantly impacting cell growth (Fig. 4*B*). In experiments where 2-hydroxy acids were supplemented to cell culture, we not

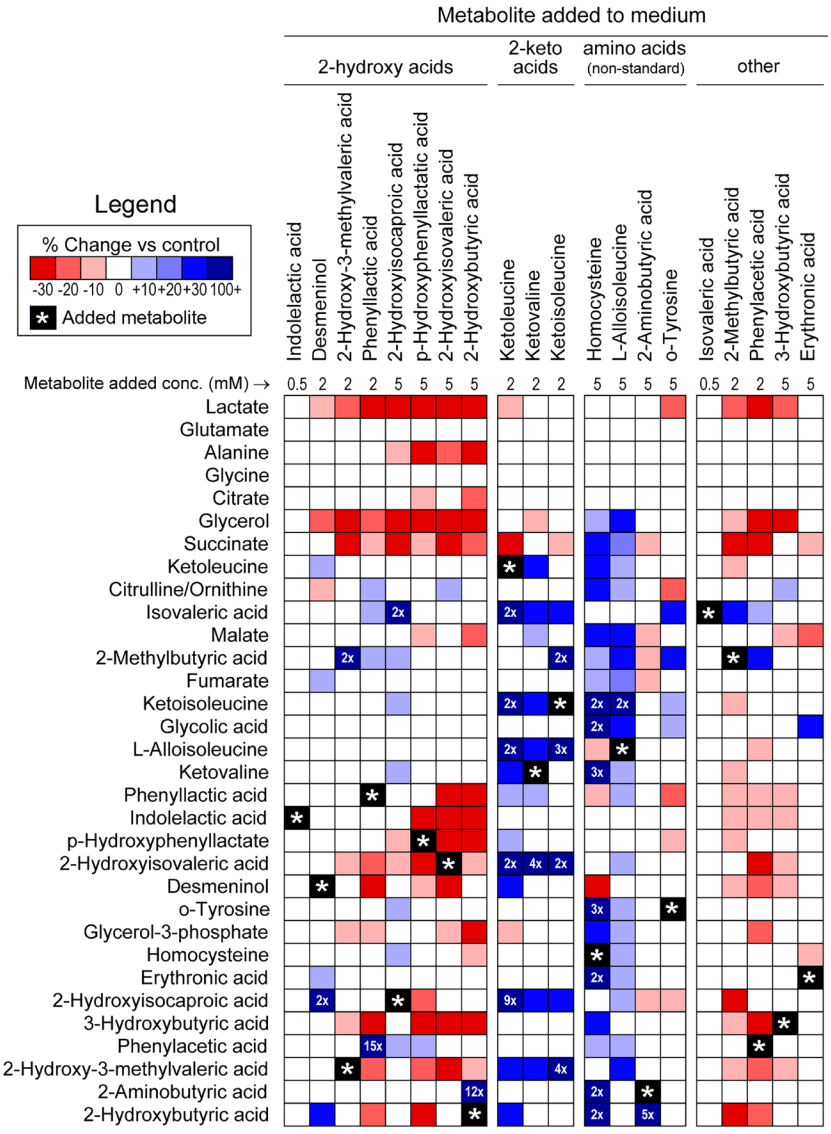

Fig. 5. Supplementation of metabolic by-products impacts secretion of other by-products. Batch cultures were performed with CHO-K1 cells, where one of 20 metabolic by-products was added to the culture at a nontoxic level. At the end of the batch culture, medium analysis was performed by GC-MS to quantify the levels of other secreted metabolic by-products and the results were compared against control experiments without any metabolites added.

only observed reduced lactate production, but also reduced the accumulation of other 2-hydroxy acids (Fig. 5 and *SI Appendix*, Fig. S1). Moreover, supplementation with 2-hydroxy acids resulted in significantly elevated levels of downstream metabolic by-products that would have required the conversion of 2-hydroxy acids to 2-keto acids. For example, supplementation with 2 mM 2-hydroxy-3-methylvaleric acid increased 2-methylbutyric acid level by twofold, supplementation with 2 mM phenyllactic acid increased phenylacetic acid level by 15-fold, supplementation with 5 mM 2-hydroxyisocaproic acid increased isovaleric acid level by twofold, and supplementation with 5 mM 2-hydroxybutyric acid increased 2-aminobutyric acid level by 12-fold (Fig. 5).

These observations let us to hypothesize that LDH could be involved in the metabolism of a broad range of 2-hydroxy acids and 2-keto acids in CHO cells. If true, this would provide a mechanism by which the identified 2-hydroxy acids could have been produced and explain reduced lactate production. To test this hypothesis, we used a commercial in vitro LDH activity assay kit to evaluate whether LDH could catalyze the conversion of nine different 2-hydroxy acids identified in this study to their respective 2-keto acids. Indeed, we found that LDH not only converted lactic acid to pyruvic acid, the native 2-hydroxy acid, and 2-keto acid substrate/product of LDH, but also converted all other eight 2-hydroxy acids to their respective 2-keto acids at high rates (Fig. 6). While these results do not rule out that other dehydrogenases may also be involved in the production of 2-hydroxy acids in CHO cell cultures, it does suggest that LDH is likely the primary enzyme involved in these conversions given its high expression in CHO cells.

Previous studies have indicated that LDH potentially acts as a redox sensor and lactate homeostasis is an integral component of redox robustness (52). In response to high NADH levels, LDH reduces pyruvate to lactate which regenerates NAD^+ (53–55). Since this reaction is reversible, LDH can be used to maintain the redox balance of the cell. Consequently, the intracellular redox state of the cell is dependent on the relative lactate and pyruvate concentrations. The ability of LDH to metabolize 2-hydroxy acids to 2-keto acids and the reduction of lactate accumulation by 2-hydroxy acids supplementation suggest that these secreted by-products may have an impact on the redox potential and cellular energy levels in CHO cell cultures. However, the impact may be blunted given their low yield in our cell cultures. Nonetheless, since lactate accumulation adversely impacts CHO cell cultures, it will be worthwhile to further investigate the role of 2-hydroxy acids supplementation in CHO cell cultures to limit lactate accumulation to and potentially enhance bioprocess performance.

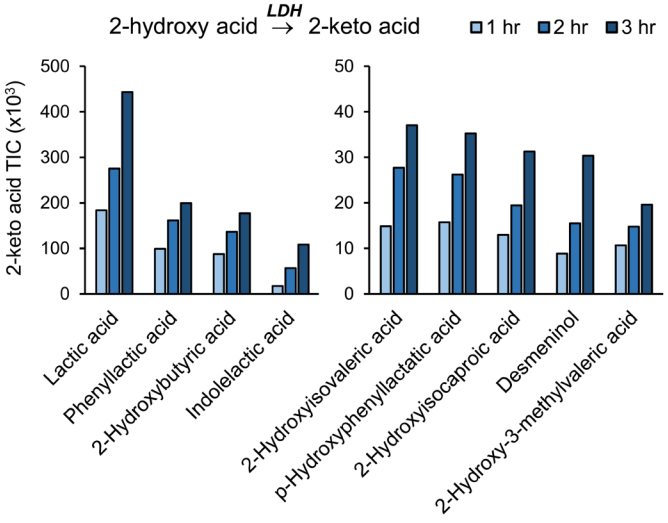

Fig. 6. LDH is a promiscuous enzyme that converts a wide range of 2-hydroxy acids to their respective 2-keto acids. An in vitro LDH assay was used with nine different 2-hydroxy acid substrates, all of which were identified as metabolic by-products in CHO cell cultures in this study. In all cases, LDH produced the expected 2-keto acid at high rates, similar to the native substrate lactic acid, as determined by GC-MS analysis.

Discussion

In this study, we have developed and applied a ubiquitously applicable stable-isotope nutrient labeling strategy together with GC-MS-based analytics and metabolomics pipeline in order to identify and track secreted metabolites emerging from amino acids and glucose that can be applied to various mammalian cell systems. With this method, we identified and verified 45 of the secreted metabolic by-products accumulating from glucose and amino acids catabolism, including a large number of previously unreported metabolites, in cell cultures from two widely used CHO cell culture systems. For the secreted by-products, we identified the nutrient sources and proposed likely enzymes involved in their production. Most of the identified metabolites originated from catabolism of glucose, BCAAs, tryptophan, tyrosine, and phenylalanine. Some of the identified metabolites, when supplemented back into CHO cell cultures at different concentrations, inhibited cell growth, while others, especially 2-hydroxy acids such as 2-hydroxyisovaleric acid, reduced lactate accumulation. In vitro enzymatic analysis indicated that all identified 2-hydroxy acids were substrates for LDH, suggesting a possible mechanism for the lowered lactate accumulation observed in our cultures. Furthermore, supplementation of some of the secreted by-products led to the increased secretion of other products. The increased secretion of some these products may be explained by the consumption of supplied metabolites via direct metabolic links, e.g., increased production of 2-methylbutyric acid, L-alloisoleucine, and 2-hydroxy-3-methylvaleric acid upon ketoisoleucine supplementation, increased production of phenylacetic acid upon supplementation of phenyllactic acid, and increased production of 2-hydroxybutyric acid upon supplementation of 2-aminobutyric acid. However, secretion of other products may have occurred due to indirect metabolic links, for example, increased production of ketoisoleucine, L-alloisoleucine, ketovaline, 2-hydroxybutyric acid, and desmeninol upon supplementation of ketoleucine (Fig. 5), and increased production of malate, fumarate, succinate, glycerol, o-tyrosine, ketovaline, citrulline/ornithine, and erythronic acid upon supplementation of homocysteine (Fig. 5). It is possible that the supplied metabolites triggered cellular responses where cells reacted to changes or fluctuations in extracellular environments and ultimately activated pathways responsible for generation of products that do not participate in the direct metabolic pathways of the supplied metabolite. For example, Harrington et al. hypothesized that catabolism of branched amino acids is linked to glycolysis and TCA cycle activities (56). Additional understanding of the direct and indirect metabolic links between these secreted by-products can help evaluate the feasibility of supplementing these by-products to overcome inefficiencies in amino acid metabolism and pave the way for genetic intervention and media reformulation strategies. Additionally, upon overlaying the findings of this study with the most recently published genome-scale model (iCHO2441) for CHO cells (57), we found that 12 out of the 45 secreted by-products and their corresponding metabolic pathways identified in our study were not included in this genome-scale model. These 12 by-products include indolelactic acid, phenyllactic acid, desmeninol, 2-hydroxy-3-methylvaleric acid, 2-hydroxyisocaproic acid, 2-hydroxyisovaleric acid, erythronic acid, isovaleric acid, 2-methylbutyric acid, o-tyrosine, L-alloisoleucine, and 2-aminobutyric acid. Out of these, desmeninol, 2-hydroxy-3-methylvaleric acid,

2-hydroxyisovaleric acid, erythronic acid, L-alloisoleucine, and 2-aminobutyric acid have not been previously reported for CHO cells. The mass balance around these secreted by-products represents constraints in the genome-scale model that will provide more realistic solutions to models relying on constraint-based optimization (flux balance analysis) especially for pathways that include the amino acid sources of the secreted by-products.

Taken together, the knowledge generated in this study can be used to modulate the accumulation of secreted by-products in mammalian cultures for biomanufacturing and other applications through altered media formulations, genetic intervention of undesirable pathways, and modification of feeding strategies of amino acids and glucose. By identifying and modulating the accumulation of secreted by-products, we can enhance the metabolic performance and physiology of mammalian cells in culture, especially for intensified processes, and implement more robust mammalian bioproduction systems for biotechnology and biomedicine.

Materials and Methods

Custom Media and Chemicals. Media and chemicals were purchased from Sigma-Aldrich (St. Louis, MO). A chemically defined CHO cell culture medium was used in this study (Sigma-Aldrich product no. 87093C). In total, 21 formulations of this medium were purchased, where in each formulation a different amino acid or glucose was omitted. The following tracers were purchased from Cambridge Isotope Laboratories: [U-^{13}C]cysteine, [U-^{13}C]histidine, [U-^{13}C]methionine, [U-^{13}C]phenylalanine, [U-^{13}C]threonine, [U-^{13}C]tryptophan, [U-^{13}C]valine, [U-^{13}C]leucine, [3,3-^{13}C]cystine, [U-^{13}C]aspartate, [U-^{13}C]glucose. The following tracers were purchased from Isotec/Sigma-Aldrich (St. Louis, MO): [U-^{13}C]arginine, [U-^{13}C]asparagine, [U-^{13}C]lysine, [U-^{13}C]proline, [U-^{13}C]tyrosine, [U-^{13}C]serine, [U-^{13}C]alanine, [U-^{13}C]glycine, [U-^{13}C]isoleucine, [U-^{13}C]glutamate, [U-^{13}C]glutamine, and [U-^{13}C]algal amino acids. To prepare ^{13}C-labeled media, an appropriate amount of ^{13}C-amino acid or ^{13}C-glucose was added to the medium that was missing the respective substrate. Media were then sterilized by filtration. To verify the identity of secreted extracellular metabolites, pure analytical standards were purchased from Sigma-Aldrich (St. Louis, MO), MOX-TBDMS derivatized, and analyzed by GC-MS. Verification was based on matching GC-MS elution time and full-scan mass spectrum.

Cell Lines and Culture Conditions. Two CHO cell lines were used in this study, a CHO-K1 suspension cell line producing IgG provided by the NIH and a GS-CHO (CHOZN®23) cell line producing IgG provided by Millipore-Sigma. For experiments performed in batch culture, CHO cells were cultured in 125 mL shake flasks with vented caps (Corning no. 431143) with 30 mL working culture volume at 125 rpm in a humidified incubator at 37 °C and 5% CO_2 (58). To prevent cell clumping in CHO-K1 cultures, 100 μL of an anticlumping agent (Gibco no. 0010057AE) was added to the medium. For CHO-K1 cultures, the medium contained 6 mM glutamine. For GS-CHO cultures, no glutamine was present in the medium. For the tracer experiments, cultures were seeded at 0.3×10^6 cells/mL and medium samples were collected on days 0 and 5 for GC-MS analysis of extracellular metabolites. For experiments with added metabolites, cultures were seeded at 0.3×10^6 cells/mL, and samples were collected daily to measure viable cell density (VCD) and glucose and lactate concentrations. Secreted extracellular metabolites were analyzed by GC-MS at the end of the cultures.

For fed-batch cultures, CHO cells were seeded at 0.3 million cells/mL in 30 mL medium and cultured in 125 mL shake flasks with vented caps (Corning no. 431143) in a humidified incubator operating at 37 °C, 125 rpm, and 5% CO_2. Feed medium for GS-CHO cells was supplemented at 5 vol% on days 3, 5, 7, 9, and 11. Glucose was supplemented up to 5.5 g/L using 45% glucose solution when the glucose levels dropped below 3 g/L. Feed medium for CHO-K1 cells was Advanced Mammalian Biomanufacturing Innovation Center (AMBIC) feed medium v1.1, which contains both glucose and amino acids. Feed medium was added daily, starting on day 4, such as to bring glucose concentration back to 5.5 g/L after feed addition. Cell culture samples were collected every 24 h. The samples were then centrifuged at 1,000 rpm to separate spent medium (supernatant) from cell pellets for further analysis.

Analytical Methods. Glucose and lactate concentrations were determined using a YSI 2700 biochemistry analyzer (YSI, Yellow Springs, OH). For the CHO-K1 cultures, VCD was quantified using a Moxi Z cell counter. For GS-CHO cultures, VCD was quantified using a hemocytometer. Cell viability was above 95% in all batch cultures, as determined by Trypan blue staining. IgG levels in spent medium were quantified on an Agilent HPLC using a protein A column (Poros 2 μm, 2.1 × 30 mm, Thermofisher, Waltham, MA).

Sample Preparation for GC-MS Analysis. To prepare samples for GC-MS analysis (59), 50 μL of medium samples were dried at room temperature under nitrogen gas flow using an evaporator (Reacti-Vap/Reacti-Therm). Next, 30 μL of 2 wt% methoxylamine hydrochloride (MOX) in pyridine solution was added and samples were incubated at 37 °C for 90 min. Finally, 50 μL of N-methyl-N-(tert-butyldimethylsilyl)-trifluoroacetamide (MTBSTFA)+1% tert-butyldimethylchlorosilane (TBDMCS) (Thermo Scientific, Bellefonte, PA) was added and samples were incubated at 60 °C for 30 min. To determine whether metabolites contained a ketone group, the MOX-derivatization step was omitted.

Gas Chromatography-Mass Spectrometry. GC-MS analysis was performed on an Agilent 7890A GC system equipped with a DB-5MS capillary column (30 m, 0.25 mm i.d., 0.25 μm-phase thickness; Agilent J&W Scientific), connected to an Agilent 5977B Mass Spectrometer operating under ionization by electron impact (EI) at 70 eV (60). Helium flow was maintained at 1 mL/min. The source temperature was maintained at 230 °C, the MS quad temperature at 150 °C, the interface temperature at 280 °C, and the inlet temperature at 250 °C. For GC-MS analysis, 1 μL was injected in splitless mode. The column was started at 80 °C for 2 min, increased to 280 °C at 7 °C/min, and held for 20 min. Data were recorded in scan mode for *m/z* between 150 and 650.

LDH In Vitro Assay. An in vitro assay was used to determine whether 2-hydroxy acids can be converted to 2-keto acids by LDH. First, individual solutions of 2-hydroxy acids (lactic acid, Sigma Cat# L7022; phenyllactic acid, Sigma Cat# P7251; 2-hydroxybutyric acid, Sigma Cat# 54917; indolelactic acid, Sigma Cat# I5508; 2-hydroxyisovaleric acid, Sigma Cat# 219835; p-hydroxyphenyllactic acid, Sigma Cat# H3253; 2-hydroxyisocaproic acid, Sigma Cat# 219827; desmeninol, Sigma Cat# PH000120; 2-hydroxy-3-methylvaleric acid, Sigma Cat# 80529) were prepared at 10 mM in water and adjusted to pH 7-8. Next, 50 μL of the 2-hydroxy acid solution was supplemented with 10 μL of LDH enzyme solution (1,000 units/mL, Sigma Cat# L3916) and 50 μL of cofactor solution (Sigma Cat# L2527 from the in vitro LDH assay kit, Sigma Cat# TOX7). The enzymatic reaction was allowed to proceed at room temperature for 1, 2, or 3 h. The reaction was stopped by addition of 20 μL of 0.1 N HCl solution. The samples were then dried at 4 °C under vacuum (Labconco CentriVap), MOX-TBDMS derivatized, and analyzed by GC-MS. The TIC of the corresponding 2-keto acids were quantified: pyruvic acid (*m/z* 174, 9.3 min), phenylpyruvic acid (*m/z* 250, 18.7 min), 2-ketobutyric acid (*m/z* 188, 10.3 min), indolepyruvic acid (*m/z* 289, 23.6 min), ketovaline (*m/z* 202, 10.9 min), 4-hydroxyphenylpyruvic acid (*m/z* 380, 26.1 min), ketoleucine (*m/z* 216, 12.4 min), 2-keto-4-methylthiobutyric acid (*m/z* 234, 16.7 min), ketoisoleucine (*m/z* 216, 12.1 min). As negative controls, assays were also performed without the addition of LDH enzyme, cofactor solution, or 2-hydroxy acids.

Data, Materials, and Software Availability. All study data are included in the article and/or supporting information.

ACKNOWLEDGMENTS. This work was funded and supported by the AMBIC through the Industry-University Cooperative Research Center Program under U.S. NSF grant number 1624684. We would like to thank Jayanth Venkatarama Reddy for discussions regarding CHO genome-scale models.

Author affiliations: [a]Department of Chemical and Biomolecular Engineering, University of Delaware, Newark, DE 19716; [b]Department of Chemical and Biomolecular Engineering, Johns Hopkins University, Baltimore, MD 21218; and [c]Department of Chemical Engineering, University of Michigan, Ann Arbor, MI 48109

Author contributions: J.E.G., H.M.N., M.J.B., and M.R.A. designed research; J.E.G., H.M.N., E.H.O., V.G.D., B.O.M., and S.K. performed research; J.E.G. and M.R.A. contributed new reagents/analytic tools; J.E.G., H.M.N., E.H.O., V.G.D., B.O.M., S.K., and M.R.A. analyzed data; and H.M.N., M.J.B., and M.R.A. wrote the paper.

1. V. G. Dhara, H. M. Naik, N. I. Majewska, M. J. Betenbaugh, Recombinant antibody production in CHO and NS0 cells: Differences and similarities. *BioDrugs* **32**, 571–584 (2018).
2. A. Verma, M. Verma, A. Singh, "Animal tissue culture principles and applications" in *Animal Biotechnology* (Academic Press, 2020), pp. 269–293.
3. R. Kojima, D. Aubel, M. Fussenegger, Building sophisticated sensors of extracellular cues that enable mammalian cells to work as "doctors" in the body. *Cell Mol. Life Sci.* **77**, 3567–3581 (2020).
4. P. Banerjee, B. Franz, A. K. Bhunia, Mammalian cell-based sensor system. *Adv. Biochem. Eng. Biotechnol.* **117**, 21–55 (2010).
5. L. E. Dow, S. W. Lowe, Life in the fast lane: Mammalian disease models in the genomics era. *Cell* **148**, 1099–1109 (2012).
6. H. M. Naik, N. I. Majewska, M. J. Betenbaugh, Impact of nucleotide sugar metabolism on protein N-glycosylation in Chinese Hamster Ovary (CHO) cell culture. *Curr. Opin. Chem. Eng.* **22**, 167–176 (2018).
7. N. Templeton, J. Dean, P. Reddy, J. D. Young, Peak antibody production is associated with increased oxidative metabolism in an industrially relevant fed-batch CHO cell culture. *Biotechnol. Bioeng.* **110**, 2013–2024 (2013).
8. C. Mohan, Y. G. Kim, J. Koo, G. M. Lee, Assessment of cell engineering strategies for improved therapeutic protein production in CHO cells. *Biotechnol. J.* **3**, 624–630 (2008).
9. G. W. Hiller, A. M. Ovalle, M. P. Gagnon, M. L. Curran, W. Wang, Cell-controlled hybrid perfusion fed-batch CHO cell process provides significant productivity improvement over conventional fed-batch cultures. *Biotechnol. Bioeng.* **114**, 1438–1447 (2017).
10. Y. Chen *et al.*, An unconventional uptake rate objective function approach enhances applicability of genome-scale models for mammalian cells. *NPJ Syst. Biol. Appl.* **5**, 25 (2019).
11. B. C. Mulukutla, J. Kale, T. Kalomeris, M. Jacobs, G. W. Hiller, Identification and control of novel growth inhibitors in fed-batch cultures of Chinese hamster ovary cells. *Biotechnol. Bioeng.* **114**, 1779–1790 (2017).
12. B. Kuang *et al.*, Identification of novel inhibitory metabolites and impact verification on growth and protein synthesis in mammalian cells. *Metab. Eng. Commun.* **13**, e00182 (2021).
13. N. W. Freund, M. S. Croughan, A simple method to reduce both lactic acid and ammonium production in industrial animal cell culture. *Int. J. Mol. Sci.* **19**, 385 (2018).
14. M. Buchsteiner, L. E. Quek, P. Gray, L. K. Nielsen, Improving culture performance and antibody production in CHO cell culture processes by reducing the Warburg effect. *Biotechnol. Bioeng.* **115**, 2315–2327 (2018).
15. W. P. Chong *et al.*, Metabolomics-driven approach for the improvement of Chinese hamster ovary cell growth: Overexpression of malate dehydrogenase II. *J. Biotechnol.* **147**, 116–121 (2010).
16. M. Zhou *et al.*, Decreasing lactate level and increasing antibody production in Chinese Hamster Ovary cells (CHO) by reducing the expression of lactate dehydrogenase and pyruvate dehydrogenase kinases. *J. Biotechnol.* **153**, 27–34 (2011).
17. D. Tang *et al.*, Preventing pyruvate kinase muscle expression in Chinese hamster ovary cells curbs lactogenic behavior by altering glycolysis, gating pyruvate generation, and increasing pyruvate flux into the TCA cycle. *Biotechnol. Prog.* **37**, e3193 (2021).
18. M. Gagnon *et al.*, High-end pH-controlled delivery of glucose effectively suppresses lactate accumulation in CHO fed-batch cultures. *Biotechnol. Bioeng.* **108**, 1328–1337 (2011).
19. B. C. Mulukutla *et al.*, Metabolic engineering of Chinese hamster ovary cells towards reduced biosynthesis and accumulation of novel growth inhibitors in fed-batch cultures. *Metab. Eng.* **54**, 54–68 (2019).
20. P. Ladiwala *et al.*, Addressing amino acid-derived inhibitory metabolites and enhancing CHO cell culture performance through DOE-guided media modifications. *Biotechnol. Bioeng.* **120**, 2542–2558 (2023).
21. M. R. Antoniewicz, G. Stephanopoulos, J. K. Kelleher, Evaluation of regression models in metabolic physiology: Predicting fluxes from isotopic data without knowledge of the pathway. *Metabolomics* **2**, 41–52 (2006).
22. J. E. Gonzalez, M. R. Antoniewicz, Tracing metabolism from lignocellulosic biomass and gaseous substrates to products with stable-isotopes. *Curr. Opin. Biotechnol.* **43**, 86–95 (2017).
23. W. S. Ahn, S. B. Crown, M. R. Antoniewicz, Evidence for transketolase-like TKTL1 flux in CHO cells based on parallel labeling experiments and (13)C-metabolic flux analysis. *Metab. Eng.* **37**, 72–78 (2016).
24. L. Wu *et al.*, Quantitative analysis of the microbial metabolome by isotope dilution mass spectrometry using uniformly 13C-labeled cell extracts as internal standards. *Anal. Biochem.* **336**, 164–171 (2005).
25. W. S. Ahn, M. R. Antoniewicz, Parallel labeling experiments with [1,2-13C]glucose and [U-13C] glutamine provide new insights into CHO cell metabolism. *Metab. Eng.* **15**, 34–47 (2013).
26. S. Nargund, J. Qiu, C. T. Goudar, Elucidating the role of copper in CHO cell energy metabolism using (13)C metabolic flux analysis. *Biotechnol. Prog.* **31**, 1179–1186 (2015).
27. G. Zhang, T. A. Neubert, Use of stable isotope labeling by amino acids in cell culture (SILAC) for phosphotyrosine protein identification and quantitation. *Methods Mol. Biol.* **527**, 79–92 (xi (2009).).
28. X. Wang *et al.*, SILAC-based quantitative MS approach for real-time recording protein-mediated cell-cell interactions. *Sci. Rep.* **8**, 8441 (2018).
29. M. R. Antoniewicz, A guide to (13)C metabolic flux analysis for the cancer biologist. *Exp. Mol. Med.* **50**, 1–13 (2018).
30. T. Fuhrer, E. Fischer, U. Sauer, Experimental identification and quantification of glucose metabolism in seven bacterial species. *J. Bacteriol.* **187**, 1581–1590 (2005).
31. L. T. Cordova, R. M. Cipolla, A. Swarup, C. P. Long, M. R. Antoniewicz, (13)C metabolic flux analysis of three divergent extremely thermophilic bacteria: Geobacillus sp. LC300, Thermus thermophilus HB8, and Rhodothermus marinus DSM 4252. *Metab. Eng.* **44**, 182–190 (2017).
32. M. R. Antoniewicz, Parallel labeling experiments for pathway elucidation and 13C metabolic flux analysis. *Curr. Opin. Biotechnol.* **36**, 91–97 (2015).
33. N. Grankvist *et al.*, Profiling the metabolism of human cells by deep (13)C labeling. *Cell Chem. Biol.* **25**, 1419–1427.e4 (2018).
34. C. P. Long, M. R. Antoniewicz, High-resolution (13)C metabolic flux analysis. *Nat. Protoc.* **14**, 2856–2877 (2019).
35. C. A. Sellick *et al.*, Metabolite profiling of recombinant CHO cells: Designing tailored feeding regimes that enhance recombinant antibody production. *Biotechnol. Bioeng.* **108**, 3025–3031 (2011).
36. N. Ma *et al.*, A single nutrient feed supports both chemically defined NS0 and CHO fed-batch processes: Improved productivity and lactate metabolism. *Biotechnol. Prog.* **25**, 1353–1363 (2009).
37. S. Dietmair *et al.*, Metabolite profiling of CHO cells with different growth characteristics. *Biotechnol. Bioeng.* **109**, 1404–1414 (2012).
38. N. Carinhas *et al.*, Metabolic signatures of GS-CHO cell clones associated with butyrate treatment and culture phase transition. *Biotechnol. Bioeng.* **110**, 3244–3257 (2013).
39. A. L. Lehninger, H. C. Sudduth, J. B. Wise, D-beta-Hydroxybutyric dehydrogenase of muitochondria. *J. Biol. Chem.* **235**, 2450–2455 (1960).
40. J. K. Stewart, D. J. Koerker, C. J. Goodner, Effects of branched-chain amino acids on postprandial 3-OH butyrate and glucagon in the baboon. *Metabolism* **37**, 405–410 (1988).
41. F. Collard *et al.*, A conserved phosphatase destroys toxic glycolytic side products in mammals and yeast. *Nat. Chem. Biol.* **12**, 601–607 (2016).
42. K. H. Telu *et al.*, Creation and filtering of a recurrent spectral library of CHO cell metabolites and media components. *Biotechnol. Bioeng.* **118**, 1491–1510 (2021).
43. O. A. Mamer, M. L. Reimer, On the mechanisms of the formation of L-alloisoleucine and the 2-hydroxy-3-methylvaleric acid stereoisomers from L-isoleucine in maple syrup urine disease patients and in normal humans. *J. Biol. Chem.* **267**, 22141–22147 (1992).
44. M. M. Dcona, B. L. Morris, K. C. Ellis, S. R. Grossman, CtBP- an emerging oncogene and novel small molecule drug target: Advances in the understanding of its oncogenic action and identification of therapeutic inhibitors. *Cancer Biol. Ther.* **18**, 379–391 (2017).
45. Y. Achouri, G. Noel, E. Van Schaftingen, 2-Keto-4-methylthiobutyrate, an intermediate in the methionine salvage pathway, is a good substrate for CtBP1. *Biochem. Biophys. Res. Commun.* **352**, 903–906 (2007).
46. C. Brocker, C. Carpenter, D. W. Nebert, V. Vasiliou, Evolutionary divergence and functions of the human acyl-CoA thioesterase gene (ACOT) family. *Hum. Genomics* **4**, 411 (2010).
47. M. C. Hunt, M. I. Siponen, S. E. Alexson, The emerging role of acyl-CoA thioesterases and acyltransferases in regulating peroxisomal lipid metabolism. *Biochim. Biophys. Acta* **1822**, 1397–1410 (2012).
48. D. E. Matthews, E. Ben-Galim, M. W. Haymond, D. M. Bier, Alloisoleucine formation in maple syrup urine disease: Isotopic evidence for the mechanism. *Pediatr. Res.* **14**, 854–857 (1980).
49. S. Ishimitsu, S. Fujimoto, A. Ohara, In vivo studies on the formation of m-tyrosine and o-tyrosine from L-phenylalanine in rats. *Chem. Pharm. Bull. (Tokyo)* **34**, 768–774 (1986).
50. S. Ishimitsu, S. Fujimoto, A. Ohara, Formation of m-tyrosine and o-tyrosine from L-phenylalanine in various tissues of rats. *Chem. Pharm. Bull. (Tokyo)* **33**, 3887–3892 (1985).
51. B. R. Ipson, A. L. Fisher, Roles of the tyrosine isomers meta-tyrosine and ortho-tyrosine in oxidative stress. *Ageing Res. Rev.* **27**, 93–107 (2016).
52. M. Luginsland, C. Kontoravdi, A. Racher, C. Jaques, A. Kiparissides, Elucidating lactate metabolism in industrial CHO cultures through the combined use of flux balance and principal component analyses. *Biochem. Eng. J.* **202**, 109184 (2024).
53. F. Hartley, T. Walker, V. Chung, K. Morten, Mechanisms driving the lactate switch in Chinese hamster ovary cells. *Biotechnol. Bioeng.* **115**, 1890–1903 (2018).
54. R. P. Nolan, K. Lee, Dynamic model of CHO cell metabolism. *Metab. Eng.* **13**, 108–124 (2011).
55. W. S. Ahn, M. R. Antoniewicz, Towards dynamic metabolic flux analysis in CHO cell cultures. *Biotechnol. J.* **7**, 61–74 (2012).
56. C. Harrington *et al.*, Production of butyrate and branched-chain amino acid catabolic byproducts by CHO cells in fed-batch culture enhances their specific productivity. *Biotechnol. Bioeng.* **118**, 4786–4799 (2021).
57. B. Strain, J. Morrissey, A. Antonakoudis, C. Kontoravdi, How reliable are Chinese hamster ovary (CHO) cell genome-scale metabolic models? *Biotechnol. Bioeng.* **120**, 2460–2478 (2023).
58. H. M. Naik *et al.*, Chemical inhibitors of hexokinase-2 enzyme reduce lactate accumulation, alter glycosylation processing, and produce altered glycoforms in CHO cell cultures. *Biotechnol. Bioeng.* **120**, 2559–2577 (2023).
59. E. H. Oates, M. R. Antoniewicz, (13)C-Metabolic flux analysis of 3T3-L1 adipocytes illuminates its core metabolism under hypoxia. *Metab. Eng.* **76**, 158–166 (2023).
60. E. H. Oates, M. R. Antoniewicz, Coordinated reprogramming of metabolism and cell function in adipocytes from proliferation to differentiation. *Metab. Eng.* **69**, 221–230 (2022).